Buckling analysis of continuous welded rail track

M.A. Van
Technical University Delft, Department of Civil Engineering, Mechanics and Structures Group, Stevinweg 1, 2628 CN Delft, The Netherlands (in detachment from Delft Geotechnics)

Continuous welded rail track, compared to jointed track not only reduces maintenance costs, but also increases life time of track components and the comfort of passengers. Since expansion of the rails is hardly possible in CWR-track, a temperature increase will result in high compressive stresses and track buckling may occur. Therefore the 'European Railway Research Institute' commissioned Delft University of Technology to develop a computer program, by which the stability of CWR on plain track and on bridges can be modelled and calculated in three directions. The computer program is called CWERRI and will be a major tool for railway companies for the implementation of new safety concepts. It further will be used for the revision of the Leaflet 720R, which code prescribes the laying and maintenance of CWR-track.

In this paper the stability of a track model is investigated. It is shown how the parameters of this track model can be derived from measurements. A sensitivity analysis is performed to determine the most significant parameters affecting the stability. It is concluded that the curvature, the horizontal ballast strength and the misalignment are the important buckling parameters. Only the very stiff fasteners improve the track stability considerably. Low fastener stiffnesses and the longitudinal and lateral ballast stiffness are less significant.

Key Words: CWR-track, Buckling, Safety concept, Measurements, Sensitivity Analysis.

1 Introduction

The last 20 years most of the jointed track in the Netherlands and in almost all other western countries, is replaced by so-called continuous welded rail (CWR) track. The rails are welded in a factory in sections with a length up to 360 m and after laying in the track, the sections are welded together. This procedure results in long tracks in which expansion is prevented. Near bridges and switches expansion joints are often used because of the complexity of the stresses and deformations if CWR would be used here. If these stresses and deformations can be predicted accurately, the expensive and uncomfortable expansion joints can be avoided.

The track is laid such that the stresses in the rails are zero at a so-called neutral temperature of approximately 25 degrees Celsius. Temperatures down to –20 degrees Celsius over the total cross-section will result in tension stresses. At low temperatures brittle rails breakage can occur what results in gaps. The gap size has to be limited to prevent derailments. At high rail temperatures, up

to 70 degrees Celsius, compressive stresses will occur in the rails. High rail temperatures are more dangerous since rail buckling can occur. Then over a length of around 20 m the track can move up to 1 m in lateral direction as can be seen in Fig. 1. The deformation mostly has a sine-form. During hot summers several hundreds of track bucklings may occur world wide [1].

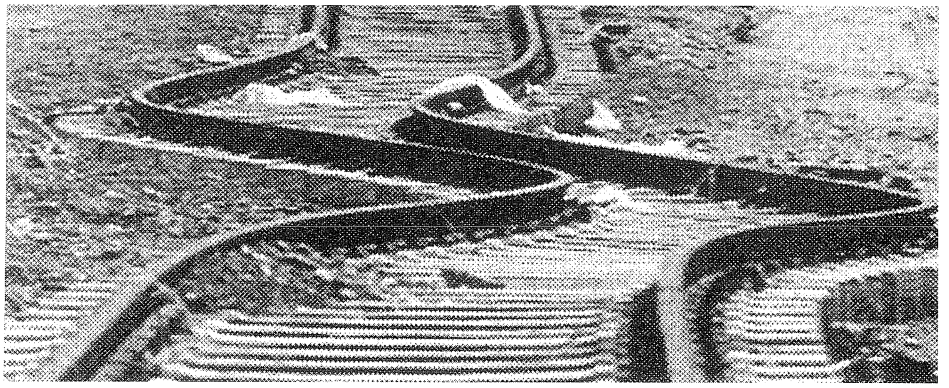

Fig. 1. Track buckle.

In 1993 the ERRI organisation (European Railway Research Institute) started a four year research program (D202-committee) to advise on the stability of CWR. Delft University of Technology has been commissioned to develop a computer program, by which the stability of CWR in plain track and on bridges can be modelled and calculated in three directions [2]. The computer program is called CWERRI and will be running on a PC in a user-friendly Windows environment. The calculation kernel of CWERRI is based on the discrete element program TILLY. The railway companies will use the program for the implementation of safety concepts for CWR-track and ERRI for the revision of Leaflet 720R, which code prescribes the laying and maintenance of CWR-track.

In this paper a track buckling model analysed with CWERRI will be presented. After presenting the model it is shown how the relevant model parameters can be derived from experimental measurements and some test results from literature are shown. Then a sensitivity analysis on buckling of curved track is performed with respect to parameters as:

- curve radius;
- peak and limit resistance of the lateral ballast strength;
- peak and limit deformation of the lateral ballast strength;
- longitudinal resistance of the ballast;
- the torsional stiffness of the fasteners;
- the amplitude and half-wave length of a misalignment.

Some remarks on safety concepts and conclusions will be given at the end of this paper.

2 Track buckling model and its parameters

In this section the track buckling model and its relevant track parameters are described. Some measurements of torsional fastener stiffness as well as longitudinal and lateral ballast behaviour are presented to found the schematisations in the model.

Track buckling mostly occurs in the horizontal plane although also vertical buckling has been observed in the past. Buckling is caused by a thermal load (ΔT) and / or mechanical loading which results in high compressive forces (see Fig. 2). If the track is perfectly straight no buckling can take place but a small misalignment (imperfection) can trigger it. The temperature, mechanical loading and the misalignment are responsible for a force in lateral (Y) direction. This force is mainly opposed by the lateral resistance of the sleeper moving in the ballast, see Fig. 3.

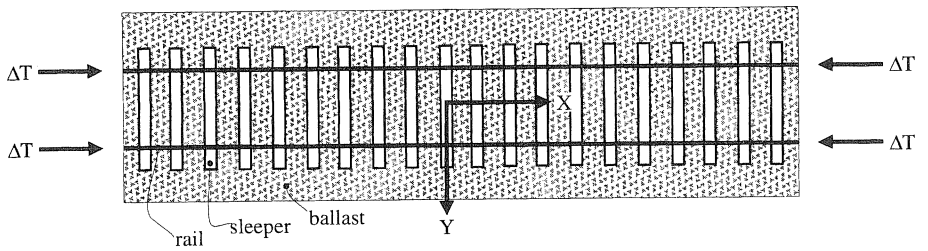

Fig. 2. Top view of track.

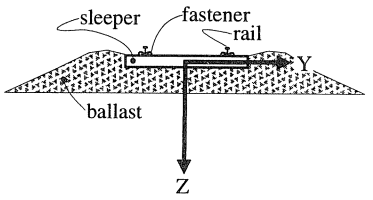

Fig. 3. Vertical plane.

Fig. 1 shows that the deformations after buckling are large. Therefore it is important to chose a geometrical non-linear beam model for the two rails. Then more realistic forces can be calculated in the deformed and buckled model. The cross-sectional area, the Young's modulus, the moment of inertia and the thermal expansion coefficient of the rail are important parameters. These parameters are known for a certain rail profile. As long as the gauge, i.e. the distance between the two rails is more or less constant and unequal shifting of the rail in the fasteners in longitudinal (X) direction is prevented, both rails can be modelled by a single beam.

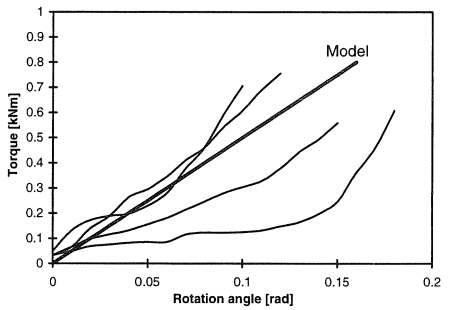

Fig. 4. Four typical torsional fasteners test data.

The fasteners resist rotation and longitudinal slip of the rail relative to the sleeper. Experimental tests can be performed to measure the torsional moment in the fastener versus the rotation angle. In such a test the rail is clamped by fasteners on a fixed sleeper and loaded by a torsional moment. Fig. 4 shows some typical data from these measurements [3].
In this study the fasteners are modelled as linear-elastic. In Chapter 3 it is shown that the computation results are only weakly dependent on the fastener stiffness.

If vertical axle loads are applied on the rails, the sleeper will move vertically in the ballast. The most simple way to model this are vertical linear-elastic springs, known as a Winkler foundation.
The static vertical deformations due to four axle loads on a Winkler foundation are shown in Fig. 5. The vertical deformation of the rail has to be limited to avoid fatigue of the rails. This requirement results in a minimum vertical stiffness of the foundation layers below the track. A typical value for the vertical spring stiffness is 100 kN/mm per meter track.

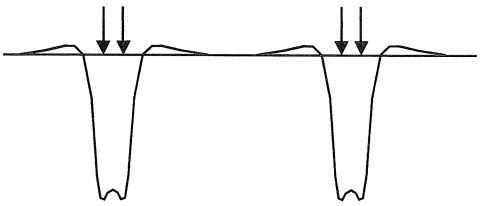

Fig. 5. Vertical deformation due to four axle loads on a beam with a Winkler foundation.

The longitudinal ballast resistance can be measured by pulling or pushing a single sleeper or a section of the track in longitudinal direction. The longitudinal deformation of the test panel and the force in the loading device are monitored. Examples of test results for tamped and consolidated track are given in Fig. 6. The figure shows that consolidation, due to vibrations of passing trains, will increase the longitudinal yield strength. The longitudinal sleeper-ballast behaviour is modelled elasto-plasticaly as shown with the thick line in Fig. 6.

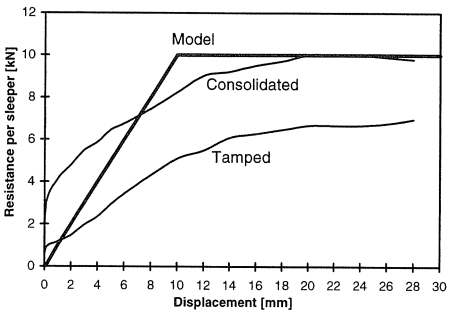

Fig. 6. Typical longitudinal ballast resistance.

The lateral behaviour of the track can be measured by pushing or pulling a track panel or one sleeper in lateral direction. A typical results of a single sleeper pushing test in consolidated and tamped track is presented in Fig. 7. Due to vibrations the gravel is compacted and the ballast resistance increases. After some displacement the density of the initially compacted gravel will decrease and the resistance will drop.

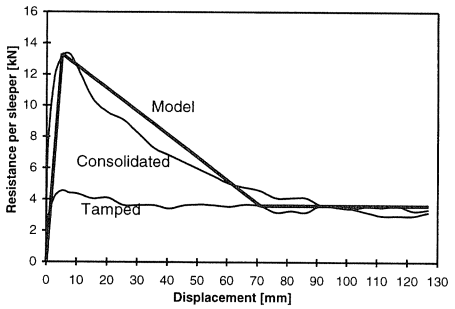

Fig. 7. Typical lateral ballast resistance.

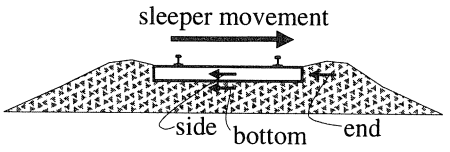

Fig. 8. Contributions to lareral ballast resistance.

The lateral sleeper resistance, as shown in Fig. 7, is a combination of the resistance of the sleeper side, end and bottom, see Fig. 8. Each contributing for approximately 1/3 of the total resistance for unloaded track (i.e. no axle loads). Vertical stresses between sleeper and ballast as a result of vertical axle loadings (see also Fig. 5) are in- or decreasing the lateral ballast resistance at the bottom of the sleeper. Measurements [4] confirm that the relation between vertical stress and lateral resistance can

be assumed linear. The lateral ballast model, which will be used for the different vertical loadings, is shown in Fig. 9.

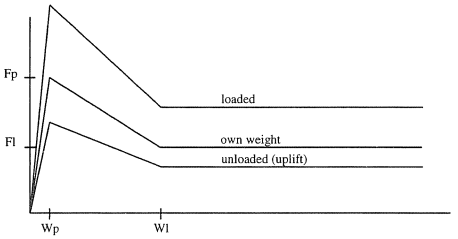

Fig. 9. Influence of vertical force on lateral ballast resistance.

For loaded track first the vertical deformations as shown in Fig. 5, are calculated. Multiplying these deformations with the vertical ballast stiffness results in distributed vertical forces R_v between the sleepers and ballast. For each sleeper the lateral peak value F_p is calculated from equation (1).

$$F_p = F_{po} + \mu_f R_v \tag{1}$$

The value of the sleeper-ballast friction coefficient μ_f is 0.86, representing an average value for concrete ties [3]. If the value of R_v is negative, in case of an uplifted track, the minimum value of R_v is restricted to minus the self weight of the track.
The limit value of the lateral resistance F_l also depends on R_v with the same ratio as F_p, see equation (2).

$$F_l = F_{lo} \cdot \frac{F_p}{F_{po}} \tag{2}$$

3 Track model to be used in a sensitivity analysis

A sensitivity analysis is performed to investigate the important parameters in curved track buckling. The track model is shown in Fig. 10.

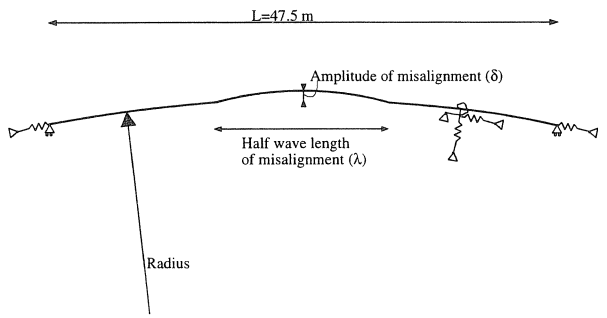

Fig. 10. Top view of track model.

The track length is 47.5 m and its curvature has a radius of 400 m. In the middle of the track a horizontal misalignment is present, characterised by a half-sine wave with a length of 9.144 meter and an amplitude of 0.0381 meter. These values are characteristic for the US-circumstances, see [3]. The rails are modelled by geometrically non-linear beam elements with the parameters of two AREA136 rails. The sleeper distance is 0.61 m. The fasteners are modelled by linear-elastic torsional springs with a spring stiffness of 111250 N/rad per m track.

In vertical direction (out of plane in Fig. 10) the track is supported by linear-elastic ballast elements with a stiffness of 68900 kN/m per meter track.

The longitudinal behaviour of the sleeper in the ballast is modelled with elasto-plastic springs in the direction of the (curved) track. The longitudinal yield strength is chosen high and longitudinal slip will not occur in the model.

Laterally the ballast is modelled with springs perpendicular to the track-axis. The constitutive behaviour of the lateral springs is given in Fig. 9. The values of F_p and F_l in this figure. are functions of the vertical stresses between the sleeper and the ballast. These stresses vary due to the vertical axle loads of the train. In case vehicle load is absent ("own weight" in Fig. 9) the value of F_{po} is 17508 N per meter track and of F_{lo} 9630 N per meter track. The lateral deformation W_p at the peak value is 0.00635 m and limit value W_l is 0.0381 m.

The model is vertically loaded by a hopper car with two boogies represented by four vertical axle loads F_v equal to 293 kN each, see Fig. 11. The centre spacing between the boogies is 12.85 meter. The spacing between the axles in a boogie is 1.78 meter. The centre of the half-sine misalignment is located in the middle between the boogies.

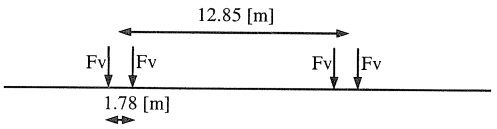

Fig. 11. Axle loads.

Additionally the track is loaded by an increase of temperature from 0 up to 100 degrees Celsius. The results of the lateral deformation in the middle of the model (between the two boogies) versus the temperature increase is shown in Fig. 12. An similar model, based on a numerical solution of a system of differential equations, gives the results of Fig. 13, see [3]. The results of the models agree very well (an increase of 100 °F is equal to 55.6 °C). The model in [3] has been validated by a number of full scale track buckling tests in the US, with and without moving trains.

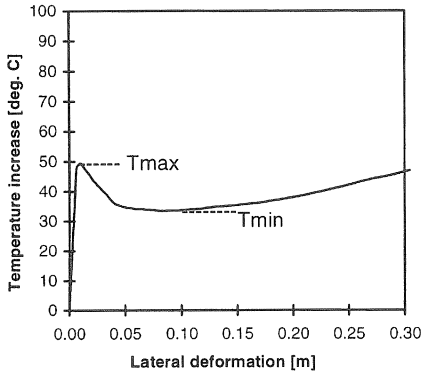

Fig. 12. Results of CWERRI.

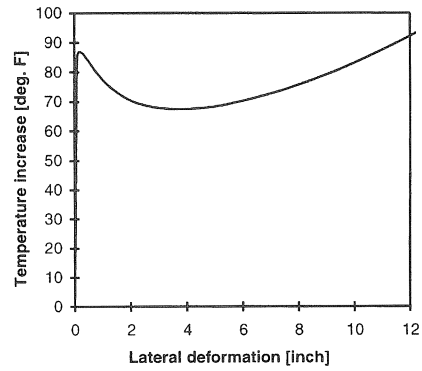

Fig. 13. Results of an equivalent model [3].

The plot of Fig. 12 or 13 can be characterised by 2 points. The first characteristic point is the temperature T_{max} at which buckling starts, which is the highest point in the figure after which the temperature will drop and deformations grow rapidly. A special developed option in CWERRI based on an arc-length controlled solver technique can follow the temperature decrease. The second characteristic point is the minimum temperature T_{min} that occurs after buckling has started. In Fig. 12 T_{max} and T_{min} are 49.4 °C and 33.5 °C respectively.

4 Results of sensitivity analysis

The sensitivity of T_{max} and T_{min} on the parameters as depicted in Table 1 will be studied. Each parameter is varied in a practical range while the other parameters are fixed. The initial values for the parameters are equal to those used in Fig. 12.

Table 1. Parameters in sensitivity study.

Parameter	Initial value	Range
Radius [m]	400	100–Tangent
Lateral peak resistance (F_p) [N per m track]	17508	8754–26262
Lateral limit resistance (F_l) [N per m track]	9630	4815–14445
Deformation peak resistance (W_p) [m]	0.00635	0.005–0.038
Deformation limit resistance (W_l) [m]	0.0381	0.00636–0.1
Longitudinal stiffness [N/m per m track]	1.378e6	1.0e5–1.0e7
Torsional stiffness [Nm/rad per m track]	1.1125e5	0.0 . 3.0e5
Amplitude of misalignment (δ) [m]	0.03821	0.008–0.05
Half-wave length of misalignment (λ) [m]	9.144	1.2–9.6

In Fig. 14 the results of the calculated T_{max} and T_{min} are shown for a varying curvature of the track. The reference value for the radius of the track is 400 m. For smaller radii the temperature at which buckling starts is decreasing. At a radius of 400 m the buckling temperature is 20 °C lower than for tangent track; at a radius of 150 m it is 20 °C lower than the value at R = 400 m. T_{min} is less sensitive.

The lateral ballast behaviour represented by both the lateral peak and limit resistance is varied over a range of 50 to 150 % of the fixed values of 17508 N/m and 9630 N/m. As expected the results vary almost linearly with these parameters, see Fig. 15. The sensitivity of T_{max} is stronger.

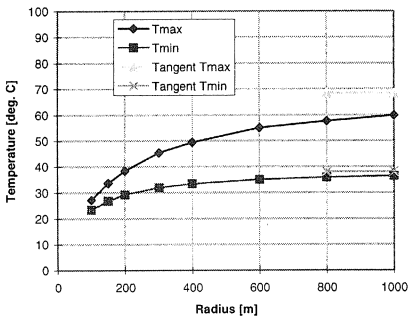

Fig. 14. ΔT versus radius.

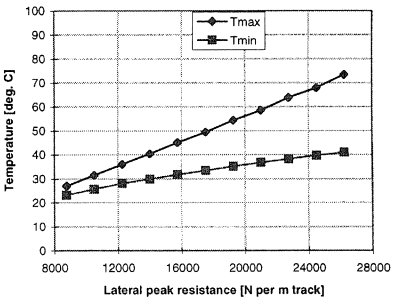

Fig. 15. ΔT versus F_p and F_l.

The influences of the deformation at peak and limit resistance are given in Fig. 16 and 17 respectively. Only small values of W_p, implying a larger initial stiffness, have some effect on T_{max}. T_{min} is less sensitive for this initial stiffness.

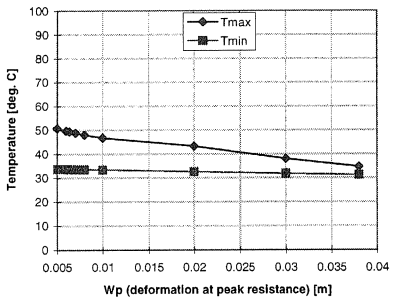

Fig. 16. ΔT versus W_p.

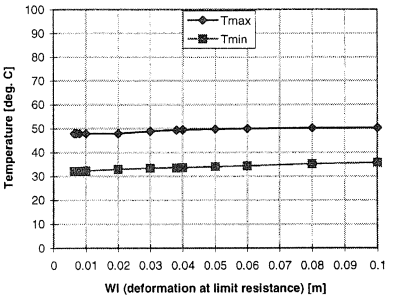

Fig. 17. ΔT versus W_l.

Variation of the longitudinal ballast-stiffness hardly influences T_{max}, see Fig. 18. This is due to the fact that at the moment that buckling starts the deformations are perpendicular to the track axis.

T_{min} is varying a little due to the fact that the geometrically non-linear track beam will generate longitudinal stresses if lateral displacements occur. These longitudinal stresses will result in some longitudinal displacements.

The torsional stiffness of the fasteners, see Fig. 19, hardly affects T_{max} or T_{min} for the range up to 3.0e5 N/rad per m track, however for spikes or Pandrol clips, as used in the USA, with torsional stiffness in the range of 6.0e5 to 1.6e6 N/rad per m track effects of this parameter are significant especially for T_{min}, which is confirmed by [3].

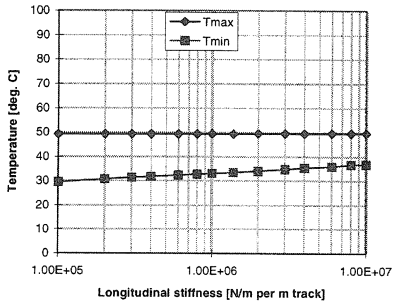

Fig. 18. ΔT versus Longitudinal stiffness.

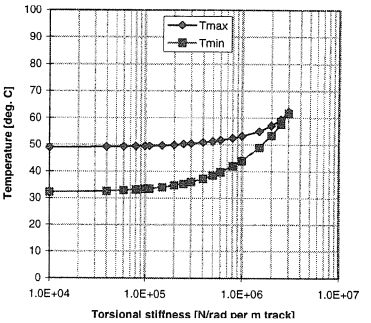

Fig. 19. ΔT versus torsional stiffness.

The amplitude of the misalignment (Fig. 20) has a significant influence on T_{max}; T_{min} is less affected.

In Fig. 21 the half-wave length is varied in combination with the amplitude of the misalignment according to the equation

$$\delta = 0.004167 \cdot \lambda \tag{3}$$

The influence on T_{max} is substantial.

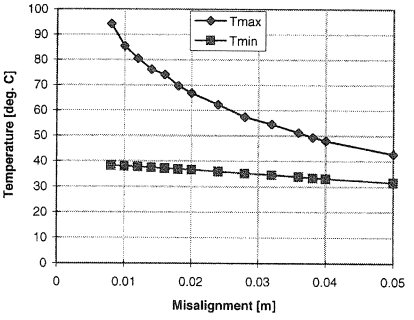

Fig. 20. ΔT versus δ.

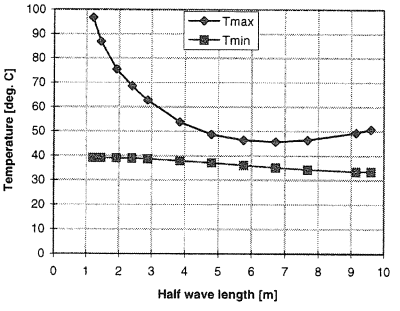

Fig. 21. ΔT versus λ.

Finally the influence of additional lateral centrifugal forces, due to the moving train, is studied. The centrifugal forces are applied at the same locations as the vertical axle loadings, see Fig. 11. The static equivalent of the centrifugal force is 57.6 kN which is 20% of the vertical axle load and representing a train velocity of 100 km/h (mass is 29300 kg per axle).
The effect of the centrifugal forces is a horizontal shift of the track. Below the axles this shift is in the direction of the misalignment, but in the middle between the boogies the track is shifting in opposite direction. Therefore the misalignment is reduced due to the centrifugal force and the calculated T_{max} and T_{min} are 2% higher for this case. This result is contrary to what is commonly believed. It should be noted that no dynamic forces are included in the model.

5 Safety concepts

Buckling starts at a temperature T_{max} after which in most cases the temperature decreases in the post buckling path (see Fig. 12). Only for weak tracks the shift is more gradual. Since T_{max} is strongly dependend on the misalignment, it can be considered as an upper bound for which buckling will occur. Following the post buckling behaviour, a minimum temperature T_{min} is found below which buckling cannot occur, which is a lower bound. Therefore, as [3] proposes, a safety criterium based on both temperatures T_{max} and T_{min} could be formulated. In case of a low ballast resistance (tamped ballast) or in case of a small track radius (curve breathing) progressive track shifting is found without a snap-through behaviour. Then T_{max} and T_{min} are not found and a criterium should be based on a limited track shifting.

6 Conclusions

The computer program CWERRI can model and calculate longitudinal, lateral and vertical forces and displacements in tracks on embankments or bridge structures. For both temperature variations and mechanical loadings the program is able to model and compute the pre- and post-buckling behaviour of continuous welded rail track.

The track buckling model consists of a geometrical non-linear beam which is vertically supported with linear elastic springs. In the horizontal plane (torsional, longitudinal and lateral direction) springs are added to model the ballast and fasteners. Measurements of the fastener rotation indicate that its behaviour can be modelled by linear-elastic springs. Measurements of the longitudinal and lateral movement of the sleeper in the ballast show different results for tamped and consolidated track. The resistance to longitudinal movements of the sleeper in the ballast is modelled with elasto-plastic springs; in lateral direction the ballast resistance is modelled with elasto-plastic springs with a softening branch for the plastic part.

A sensitivity analysis has been performed showing the significance of the different parameters in track buckling. It is concluded that for the cases investigated the curvature, the lateral ballast strength and the amplitude and half-wave length of track misalignments (imperfections) show to be

most important. The lateral and longitudinal ballast-stiffness as well as a relatively low torsional stiffness of the fasteners are less significant parameters. However a high torsional stiffness of the fasteners improves the buckling temperature considerably.

It is recommended that a safety criterium for track buckling is not only based on the maximum temperature at which buckling starts, but also on the minimum temperature after buckling. The latter temperature can be found with a post-buckling computation.

7 References

[1] DAVIDS, G.A., Federal Viewpoint, AREA Bulletin no. 683, 1981.

[2] DIETERMAN, H.A. and M.A. VAN, Dynamic stability of CWR-track, Description of the CWERRI-program, TU Delft, September 1993.

[3] SAMAVEDAM, G. , A. KISH, A. PURPLE and J. SCHOENGART, Parametric Analysis and Safety Concepts of CWR Buckling, U.S. Department of Transportation, John A. Volpe National Transportation Systems Center, Cambridge, report number DOT-VNTSC-FRA-93-25, December 1993.

[4] DIETERMAN, H.A., M.A. VAN, A.J.P. VAN DAM, C. ESVELD, Longitudinal forces in railroad structures, Rail Engineering International, Edition 1990 number 1.